

Northwest Atlantic



Fisheries Organization

Serial No. N7404

NAFO SCR Doc. 23/017

**SCIENTIFIC COUNCIL MEETING – JUNE 2023**

**Biogeochemical oceanographic conditions in the Northwest Atlantic (NAFO subareas 2-3-4) during 2022**

by

D. Bélanger<sup>1</sup>, G. Maillet<sup>1</sup>, P. Pepin<sup>1</sup>

<sup>1</sup> Fisheries and Oceans Canada, Northwest Atlantic Fisheries Centre, P.O. Box 5667, St. John's, NL, Canada, A1C 5X1

**Abstract**

This report reviews the spatiotemporal variability in biogeochemical indices derived from satellite observations (spring phytoplankton bloom initiation, duration and magnitude) and *in situ* measurement of oceanographic variables (nitrate and chlorophyll-*a* concentration, and zooplankton abundance and biomass) across NAFO Subareas 2, 3 and 4 with an emphasis on the year 2022. The initiation of the spring phytoplankton bloom was earlier than normal in the Gulf of St. Lawrence and on the Scotian Shelf, later than normal on the Grand Bank and the Flemish Cap, and near normal elsewhere. Nitrate inventories increased from near normal to above normal and were at their highest level since 2015, while chlorophyll *a* inventories remained near normal for a 2<sup>nd</sup> consecutive year. The decrease in total copepod abundance from above normal to near normal was mainly driven by a decrease in the abundance of small copepod taxa including *Pseudocalanus* spp., which was at its lowest level since 2012. A similar decrease in total zooplankton biomass from above normal to near normal was driven by a decline in the abundance of the large, energy-rich *Calanus finmarchicus* copepods which was at its lowest level since 2015.



## Table of Contents

Abstract .....	1
Table of Contents.....	2
1. Introduction.....	5
2. Methods .....	5
3. Variability in nutrient, chlorophyll <i>a</i> , and zooplankton inventories in NAFO Subareas 2 to 4 .....	6
3.1. Spring phytoplankton bloom.....	6
3.2. Nitrate and chlorophyll <i>a</i> .....	7
4. Relationships between ocean climate and biogeochemical oceanographic conditions .....	9
5. Biogeochemical oceanographic highlights for 2022.....	10
Acknowledgments .....	11
References .....	11

## List of Figures

**Figure 1.** NAFO Ecological Production Units (EPUs) used to summarize biogeochemical oceanographic conditions in the NW Atlantic. The Gulf of St. Lawrence is also used as a grouping unit although it is not an official EPU. This report does not address conditions in the Gulf of Maine, and Mid-Atlantic Bight EPUs. Figure modified from Koen-Alonso et al. 2019. .... 144

**Figure 2.** (A) Location of the boxes used to calculate spring bloom indices (initiation duration, magnitude) from satellite Ocean Color imagery: (HS=Hudson Strait, NLS=northern Labrador Shelf, CLS=central Labrador Shelf, HB=Hamilton Bank, SAB=St. Anthony Basin, NENS=northeast Newfoundland Shelf, FP=Flemish Pass, FC=Flemish Cap, NGB=northern Grand Bank, SES=southeast Shoal, SPB=Green-St. Pierre Bank, NEGSL=northeast Gulf of St. Lawrence, NWGSL=northwest Gulf of St. Lawrence, MS=Magdalen Shallows, ESS=eastern Scotian Shelf, CSS=central Scotian Shelf, WSS=western Scotian Shelf. (B) Location of Atlantic Zone Monitoring Program (AZMP) oceanographic sections (black lines: BI=Beachy Island; MB=Makkovik Bank; SI=Seal Island; BB=Bonavista Bay; FC=Flemish Cap; SEGB=Southeastern Grand Bank; TBB+TCEN+TDC=Eastern Gulf of St. Lawrence; TESL+TSI+TASO=Western Gulf of St. Lawrence; TIDM=Southern Gulf of St. Lawrence; LL=Louisbourg Line; HL=Halifax Line; BBL=Brown Bank Line), and coastal high-frequency monitoring sites (red circles: S27=Station 27; R=Rimouski; S=Shediac Valley; H2=Halifax 2; P5=Prince 5) where biogeochemical data (nitrate, chlorophyll *a*, zooplankton abundance and biomass) were collected..... 155

**Figure 3.** Mean values  $\pm 0.5$  SD (rectangles) and  $\pm 1$  SD (whiskers) for the spring phytoplankton bloom (A) initiation, (B) duration, and (C) magnitude derived from ocean colour satellite data over the 2003-2020 reference period. The three parameters were calculated for six NAFO Ecological Production Units (EPUs: Labrador Shelf, Newfoundland Shelf, Flemish Cap, Grand Bank, Southern Newfoundland, Scotian Shelf) and for the Gulf of St. Lawrence. See Fig. 1 for EPU locations. .... 166

**Figure 4.** Annual standardized anomaly scorecards for the spring phytoplankton bloom (A) initiation, (B) duration, and (C) magnitude for seven NAFO Ecological Production Units (EPU) and for the Gulf of St. Lawrence (GSL). Standardized anomalies were calculated for each oceanographic section and high-frequency monitoring site using a 2003-2020 reference period and averaged over geographical grouping units (EPUs or GSL). Red (blue) cells indicate later (earlier) bloom initiation, longer (shorter) bloom duration, or higher (lower) bloom magnitude relative to the 2003-2020 reference period. White cells indicate near-normal conditions, i.e.  $\pm 0.5$  SD from the mean for the reference period. Grey cells indicate years for which limited

data availability did not permit index calculation. Regions are listed from North (top) to south (bottom). See Fig. 1 for the location of geographical grouping units. .... 177

**Figure 5.** Annual anomaly time series of (A) 50-150 m integrated nitrate, and (B) 0-100 m integrated chlorophyll-*a* inventories in six NAFO Ecological Production Units (EPU) and in the Gulf of St. Lawrence (GSL). Standardized anomalies were calculated for each oceanographic section and high-frequency monitoring site using a 1999-2020 reference period and averaged over geographical grouping units (EPUs or GSL). White circle indicate the mean annual anomaly for the Northwest Atlantic (NWA). Colour bars indicate the relative contribution of each grouping unit to the mean anomaly. The black line is a loess regression fitted to the annual mean anomalies that summarizes the broad-scale temporal trend observed across the NWA. See Figs. 1 & 2B for the location of geographical grouping units, oceanographic sections and high-frequency monitoring sites. .... 188

**Figure 6.** Comparison between 2021 and 2022 annual anomalies of (A) 50-150 integrated nitrate, and (B) 0-100 m integrated chlorophyll-*a* inventories for each AZMP oceanographic section and high-frequency monitoring site sampled by the AZMP. Anomalies were calculated based on a 1999-2020 reference period. Anomalies within  $\pm 0.5$  SD (vertical dashed lines) are considered to represent near-normal conditions. Sampling locations are listed from north (top) to south (bottom). Asterisks (\*) indicate high-frequency monitoring sites. See Figure 2B for oceanographic sections and high-frequency monitoring sites location. ... 199

**Figure 7.** Anomaly time series of (A) copepod, and (B) non-copepod zooplankton abundance ( $\text{ind.} \cdot \text{m}^{-2}$ ) in six NAFO Ecological Production Units (EPU) and in the Gulf of St. Lawrence (GSL). Standardized anomalies were calculated for each oceanographic section and high-frequency monitoring site using a 1999-2020 reference period and averaged over geographical grouping units (EPUs or GSL). White circle indicate the mean annual anomaly for the Northwest Atlantic (NWA). Colour bars indicate the relative contribution of each grouping unit to the mean anomaly. The black line indicate the overall trend across the NWA based on 3-y running average of annual mean anomalies. See Figs. 1 & 2B for the location of geographical grouping units, oceanographic sections and high-frequency monitoring sites. .... 20

**Figure 8.** Comparison between 2021 and 2022 annual anomalies for copepod (A), and non-copepod (B) abundance ( $\text{ind.} \cdot \text{m}^{-2}$ ) for each AZMP oceanographic section and high-frequency monitoring site sampled by the AZMP. Anomalies are calculated based on a 1999-2020 reference period. Anomalies were calculated based on a 1999-2020 reference period. Anomalies within  $\pm 0.5$  SD (vertical dashed lines) are considered to represent near-normal conditions. Sampling locations are listed from north (top) to south (bottom). Asterisks (\*) indicate high-frequency monitoring sites. See Figure 2B for oceanographic sections and high-frequency monitoring sites location. .... 211

**Figure 9.** Annual anomaly time series of (A) *Calanus finmarchicus* and (B) *Pseudocalanus* spp. copepod abundance ( $\text{ind.} \cdot \text{m}^{-2}$ ) in six NAFO Ecological Production Units (EPU) and in the Gulf of St. Lawrence (GSL). Standardized anomalies were calculated for each oceanographic section and high-frequency monitoring site using a 1999-2020 reference period and averaged over geographical grouping units (EPUs or GSL). White circle indicate the mean annual anomaly for the Northwest Atlantic (NWA). Colour bars indicate the relative contribution of each grouping unit to the mean anomaly. The black line indicate the overall trend across the NWA based on 3-y running average of annual mean anomalies. See Figs. 1 & 2B for the location of geographical grouping units, oceanographic sections and high-frequency monitoring sites. .... 222

**Figure 10.** Comparison between 2021 and 2022 annual anomalies for (A) *Calanus finmarchicus*, and (B) *Pseudocalanus* spp. copepod abundance ( $\text{ind.} \cdot \text{m}^{-2}$ ) for each AZMP oceanographic section and high-frequency monitoring site sampled by the AZMP. Anomalies were calculated based on a 1999-2020 reference period. Anomalies within  $\pm 0.5$  SD (vertical dashed lines) are considered to represent near-normal conditions. Sampling locations are listed from north (top) to south (bottom). Asterisks (\*) indicate high-frequency monitoring sites. See Figure 2B for oceanographic sections and high-frequency monitoring sites location. ... 233

**Figure 11.** Annual anomaly time series of zooplankton biomass ( $\text{g dry weight} \cdot \text{m}^{-2}$ ) in six NAFO Ecological Production Units (EPU) and in the Gulf of St. Lawrence. Standardized anomalies were calculated for each

oceanographic section and high-frequency monitoring site using a 1999-2020 reference period and averaged over geographical grouping units (EPUs or GSL). White circle indicate the mean annual anomaly for the Northwest Atlantic (NWA). Colour bars indicate the relative contribution of each grouping unit to the mean anomaly. The black line indicate the overall trend across the NWA based on 3-y running average of annual mean anomalies. See Figs. 1 & 2B for the location of geographical grouping units, oceanographic sections and high-frequency monitoring sites. .... 244

**Figure 12.** Comparison between 2021 and 2022 annual anomalies for zooplankton biomass ( $\text{g} \cdot \text{dry weight} \cdot \text{m}^{-2}$ ) for each AZMP oceanographic section and high-frequency monitoring site sampled by the AZMP. Anomalies are calculated based on a 1999-2020 reference period. Anomalies within  $\pm 0.5$  SD (vertical dashed lines) are considered to represent near-normal conditions. Sampling locations are listed from north (top) to south (bottom). Asterisks (\*) indicate high-frequency monitoring sites. See Figure 2B for oceanographic sections and high-frequency monitoring sites location. .... 255

**Figure 13.** Correlation matrix summarizing the relationships between physical (Newfoundland and Labrador climate index, winter North Atlantic Oscillation [NAO] index, air temperature, sea ice cover, sea surface temperature [SST], and bottom temperature), and biogeochemical (phytoplankton spring bloom initiation, duration, and magnitude; integrated deep nitrate [50-150 m]; integrated chlorophyll *a* [chl *a* 0-100 m]; abundance of copepod, non-copepod, *Calanus finmarchicus*, *Pseudocalanus* spp.; zooplankton biomass) indices for the Southern Newfoundland, Grand Bank, Flemish Cap, Newfoundland Shelf, and Labrador Shelf EPUs during the 1999-2022 period. Green cells indicate significant positive correlation, red cells indicate significant negative correlation, and white cells indicate non-significant correlations. Numbers in cells are Spearman correlation coefficients ( $\rho$ ). Significance level for Spearman correlation tests was  $\alpha=0.05$ . .... 266

## 1. Introduction

Here, we review the biogeochemical oceanographic conditions in Northwest Atlantic (NWA) shelf and slope waters within NAFO Subareas 2, 3 and 4. Data collected in 2022 are presented and referenced to archive data to provide information about broad-scale trajectories of biogeochemical metrics at annual to decadal time scales. Satellite ocean colour observations and seasonal sampling of oceanographic sections and high-frequency monitoring stations by the Atlantic Zone Monitoring Program (AZMP) provided reasonable spatial and temporal series coverage. The monitoring of standard variables (nutrients, chlorophyll *a*, and zooplankton abundance) since 1999 (AZMP) or 2003 (MODIS satellite sensor) allows to assess the spatial and temporal variability of ecologically relevant indices across the NWA. We used NAFO Ecological Production Units (EPU) and the Gulf of St. Lawrence as geographical grouping units to summarise biogeochemical indices at a scale deemed appropriate for integrated ecosystem management plans in the NWA (Koen-Alonso et al. 2019; see Fig. 1 for EPUs location). Additional details on physical, and biogeochemical oceanographic conditions in the NWA in 2022 and earlier years can be found in Ringuette et al. (2022), Maillet et al. (2022), Blais et al. (2021), Galbraith et al. (2022), Hebert et al. (2021), Cyr et al. (2022), Yashayaev et al. (2021), Casault et al. (2023).

## 2. Methods

Surface chlorophyll *a* (chl *a*) concentration was obtained from satellite observation of ocean colour by the Moderate Resolution Imaging Spectroradiometer (MODIS-Aqua) sensor (<http://modis.gsfc.nasa.gov/>). Daily mean surface chl *a* concentrations were used to characterise the phenology of the spring phytoplankton bloom (bloom initiation, duration and magnitude) over the period covered by MODIS, i.e., 2003-present. Estimates of spring bloom initiation, duration, and magnitude were obtained with the PhytoFit Shiny app (Clay et al. 2021) which uses a method adapted from shifted Gaussian function of time and a method adapted from Zhai et al. (2011) to calculate these metrics within subareas of the NWA continental shelf (see Fig. 2A for satellite boxes location).

Collection of standard AZMP variables (integrated nitrate [50-150 m] and chl *a* [0-100 m] inventories, total abundance of copepods, non-copepods, *Calanus finmarchicus* and *Pseudocalanus* spp., and zooplankton biomass) followed protocols outlined in Mitchell et al. (2002). Observations for 2022 and earlier years presented in this document are based on seasonal surveys conducted in spring (April), summer (July) and fall (November) along standard AZMP oceanographic sections and at high-frequency monitoring stations sampled at a weekly to monthly interval during the ice-free period of the year (see Fig 2B for the location of oceanographic sections and high-frequency monitoring stations). Anomalies were used to summarize spatial and temporal variability in the biogeochemical environment and at the lower trophic levels. Annual standardized anomalies were calculated for each selected variable by subtracting the mean of the reference period from the annual mean observation and by dividing the result by the standard deviation (SD) for the reference period ( $[\text{observation} - \text{mean}]/\text{SD}$ ). Anomalies for the spring bloom indices (bloom initiation and magnitude) were calculated on log-transformed ( $\ln$ ) data. Annual standardized anomalies for nitrate, chlorophyll, copepod, non-copepod, *Calanus finmarchicus*, and *Pseudocalanus* spp, and zooplankton biomass were calculated using the least square means of linear models that included the fixed factors Year, Season and Station (standard oceanographic sections) or Year and Month (High-frequency monitoring stations) fitted to log-transformed data ( $\ln(x+1)$ ). The results of this standardization yielded a series of annual anomalies that illustrate departures from the long-term average conditions, or climatology, across the range of variables. The difference between a given year and the climatological mean represents the magnitude of that departure from the reference period. The reference periods used are 2003-2020 for the spring bloom indices derived from satellite observations, and 1999-2020 for AZMP biogeochemical indices.

Anomaly values within  $\pm 0.5$  SD from the climatological mean are representative of near-normal conditions. Positive anomalies  $> 0.5$  SD indicate conditions above (or later for bloom initiation) the climatological mean. Negative anomalies  $< 0.5$  SD indicate conditions below (or earlier for bloom initiation) the climatological mean. Annual standardized anomalies of each oceanographic section and high-frequency monitoring station were averaged over NAFO EPUs (Labrador Shelf [LS], Newfoundland Shelf [NS], Flemish Cap [FC], Grand Bank

[GB], Southern Newfoundland [SN], Scotian Shelf [SS]) and the Gulf of St. Lawrence to provide an estimate of mean oceanographic trends within each EPU. The variables selected were: spring bloom initiation (day of year), duration (number of days), and magnitude ( $\text{mg} \cdot \text{m}^{-3} \cdot \text{d}^{-1}$ ); 50-150 m integrated nitrate ( $\text{mmol} \cdot \text{m}^{-2}$ ); 0-100 m integrated chlorophyll *a* ( $\text{mg} \cdot \text{m}^{-2}$ ); copepod, non-copepod, *Calanus finmarchicus*, and *Pseudocalanus* spp. abundance ( $\text{ind.} \cdot \text{m}^{-2}$ ); and total zooplankton biomass ( $\text{g} \cdot \text{dry weight} \cdot \text{m}^{-2}$ ). To estimate broad-scale spatial trends across the NWA, a weighted mean anomaly index was calculated for each sampling year by summing the annual anomalies of each AZMP oceanographic section and high-frequency monitoring station, and dividing the result by the total number of sections and stations included in the calculation.

We produced a Pearson correlation matrix to quantify the strength of the relationships between the various biogeochemical indices presented above and the physical environment using the ocean climate index developed by Cyr and Galbraith (2021) for the Newfoundland and Labrador region. We used annual anomalies of the composite climate index and of a subset of its components, namely the winter NAO index, air temperature, sea ice extent, sea surface temperature, and bottom temperature. Biogeochemical anomalies from the Scotian Shelf and the Gulf of St. Lawrence were not included in the calculation of the correlations because these regions are not covered by the climate index.

Limited availability of satellite data in the spring because of cloud and/or sea ice cover did not permit reliable calculations of the spring phytoplankton bloom metrics for the central and northern Labrador boxes. Moreover, unavailability of scientific research vessels resulted in the cancellation of the summer survey in the Newfoundland Region and the Makkovik Bank and Beachy Island sections were not sampled. Consequently, indices for the Labrador Shelf EPU derived from satellite observations or *in situ* measurements during oceanographic surveys are not presented in this report for the year 2022.

### 3. Variability in nutrient, chlorophyll *a*, and zooplankton inventories in NAFO Subareas 2 to 4

#### 3.1. Spring phytoplankton bloom

The initiation of the spring phytoplankton bloom in eastern Canadian shelf waters occurs earlier in the south compared to regions to the north. On average, the spring bloom begins between late March and early of April on the Scotian Shelf, Gulf of St. Lawrence, Southern Newfoundland, Grand Bank, and the Flemish Cap (Fig. 3A). Bloom initiation typically occurs in mid-to-late April on the Newfoundland Shelf, and up to one month later on the Labrador Shelf where extensive sea ice cover delays the initiation of the bloom. Spring bloom initiation timing was variable across the NWA throughout the 20-year time series with no clear spatial or temporal trend except for 2010 when blooms were notably earlier across the region (Fig. 4A). Bloom initiation in the NWA was mainly near or earlier than normal across the region from 2004 to 2006, and mainly later than normal from 2014 to 2017 (Fig. 4A). In 2022, spring bloom initiation was, on average, earlier than normal in the Gulf of St. Lawrence and on the Scotian Shelf, near normal in Southern Newfoundland and on the Newfoundland Shelf, and later than normal on the Flemish Cap and the Grand Bank where late blooms were observed for a third consecutive year (Fig. 4A).

The duration of the spring bloom generally increases with latitude from ~25-40 days Scotian Shelf, to ~45-60 days on the Newfoundland Shelf (Fig. 3B). The duration of the bloom is longest and more variable on the Flemish Cap where it can last anywhere between ~60 and 95 days. Delayed bloom onset on the Labrador shelf generally results in slightly shorter duration (~35-55 days) compared to the Newfoundland Shelf (Fig. 3B). Bloom duration was variable throughout the time series with no clear broad-scale spatial or temporal trend (Fig. 4B). In 2022, bloom duration was, on average, shorter than normal in Southern Newfoundland and on the Grand Bank and the Newfoundland Shelf, and near normal elsewhere (Fig. 4B). Overall, spring bloom duration has been mainly near normal or slightly shorter than normal across the NWA since 2020 (Fig. 4B).

The magnitude of the spring bloom is a function of bloom duration and bloom intensity, i.e., the surface chlorophyll concentration at given point in time. It varies considerably among EPUs, being lowest in the Labrador Shelf and in the Southern Newfoundland, highest on the Flemish Cap, Grand Bank and Gulf of St. Lawrence, and intermediate on the Scotian Shelf and the Newfoundland Shelf (Fig. 3C). Spring bloom

magnitude was variable across the NWA between 2003 and 2011. It remained mainly near or slightly lower than normal from 2011 through 2017, before increasing to mainly above-normal levels in 2018 and 2019 (Fig. 4C). Several higher-than-normal magnitudes have been observed in the southernmost regions (Scotian Shelf, Gulf of St. Lawrence and Southern Newfoundland) since 2020, while magnitude has remained mainly near or below normal elsewhere during the same period (Fig. 4C). In 2022, bloom magnitude was below normal for a second consecutive year on the Grand Bank, near normal in the Gulf of St. Lawrence and on Flemish Cap and the Newfoundland Shelf, and above normal in Southern Newfoundland and on the Scotian Shelf where magnitude was above the long-term average for a 2<sup>nd</sup> consecutive year (Fig 4C).

### 3.2. Nitrate and chlorophyll *a*

Mean annual anomalies of integrated (50-150 m) nitrate inventories decreased from near-to-above normal levels during the 2000s to mainly near-to-below normal levels during the 2010s (Fig. 5A). Nitrate inventories have been generally increasing across the NWA since 2018 and reached an overall above-normal level in 2022 for the first time since 2015 (Fig. 5A). In 2022, nitrate inventories were mainly above normal on the Newfoundland Shelf and the Grand Bank with a notable increase at Station 27 compared to the previous year (Fig. 6A). Despite the above-normal levels observed in the Central GSL and the Cabot Strait, nitrate inventories were generally low in the Gulf of St. Lawrence with levels <2 standard deviations below the long-term average along the Eastern GSL section and at the Rimouski and Shediac Valley high-frequency stations (Fig 6A). On the Scotian Shelf, nitrate inventories remained above normal at the Halifax 2 station (4W) but decreased from above normal to near normal along the Halifax (4W) and Louisbourg (4Vs) sections, and from near normal to below normal at the Prince 5 station in the Bay of Fundy (4X) compared to the previous year (Fig. 6A).

Integrated chl *a* (0-100 m) and nitrate (50-150 m) inventories show similar overall temporal trend with periods of higher nitrate levels corresponding to higher chlorophyll inventories and vice versa (Fig. 5A, B). Concordance between broad-scale nitrate and chlorophyll trends is not surprising given that nitrate is one of the main limiting factor of oceanic primary production (Bristow et al. 2017). Mean annual anomalies indicated near-normal chl *a* levels during the 2000s, and near or below normal levels from 2011 through 2016 when chl *a* inventories were at a record-low level (Fig. 5B). Chl *a* inventories have since increased to near or above normal levels (Fig 5B). In 2022, chl *a* inventories were above normal on the Newfoundland Shelf, which represented an increase compared to the near-normal and below-normal levels of the previous year for the Seal Island (2J) and Bonavista (3K) sections, respectively (Fig. 6B). Inventories were below normal across the Grand Bank (3LNO) and the Flemish Cap (3M), which represented a decrease compared to the near-normal levels observed during the previous year. In the Gulf of St. Lawrence, inventories were above normal everywhere except for the below-normal levels observed in the Northwest GSL (4ST) and at the Shediac Valley (4T), while inventories were either near normal or above normal on the Scotian Shelf with the exception of the below- normal level observed at Prince 5 station (4X) in the Bay of Fundy (Fig 6B).

### 3.3 Zooplankton abundance and biomass

Copepods numerically dominate zooplankton assemblages in Canadian shelf waters (Maillet et al. 2022, Casault et al., 2023, Blais et al. 2021). Mean copepod abundance increased from below normal to above normal between 2000 and 2010 before stabilizing at near-normal levels during the 2010s (Fig 7A). Mean copepod abundance was high in 2020 and 2021, but decreased in 2022, reaching its lowest level in 20 years (Fig 7A). The most important decrease in 2022 compared to the previous year occurred on the Bonavista section (3K) and in the 3M part of the Flemish Cap where copepod abundance went from above normal in 2021 to below normal in 2022 (Fig 8A). Copepod abundance in the Gulf of St. Lawrence remained above normal in 2022 in the eastern GSL (4RS) and at the Rimouski (4T) and Shediac Valley (4T) stations and below normal in the northwest GSL (4ST) while increasing from below normal to near normal in the central GSL (4RST) (Fig. 8A). On the Scotian Shelf, copepod abundance in 2022 remained below normal at the Halifax 2 station (4W), near normal on the Browns Bank section (4X) and above normal in the at the Prince 5 station (4X) in the Bay of Fundy, but decreased from near normal to below normal along the Louisbourg (4Vs) and Halifax (4W) sections (Fig. 8A).

Most abundant non-copepod zooplankton taxa include appendicularians, pteropods, chaetognaths, cladocerans, cnidarians and ctenophores (Maillet et al. 2022). Mean abundance of non-copepod zooplankton across the NWA showed little variability throughout the 2000s before increasing almost steadily from below normal to above normal between 2010 and 2015 (Fig. 7B). Non-copepod abundance has remained above normal since 2015 with mostly positive anomalies for all EPUs (Fig. 7B). In 2022, the abundance of non-copepod zooplankton was mainly above normal on the Newfoundland Shelf and the Grand Bank, but decreased from above normal to near normal on the Bonavista section (3K) and the Flemish Cap (3M portion of the Flemish Cap section) as well as at Station 27 (3L) compared to the previous year (Fig. 8B). Non-copepod abundance was above normal everywhere in the Gulf of St. Lawrence in 2022 except for the below-normal level observed in the northwest GSL (4ST) (Fig. 8B). This represented an increase from the near-normal levels observed in the central GSL (4RST) and at the Shediak Valley (4T) during the previous year (Fig. 8B). On the Scotian Shelf, non-copepod abundance was near normal everywhere except for the below-normal level at the Halifax 2 station (4W) (Fig. 8B).

*Calanus finmarchicus* is a large, energy-rich, and widely distributed copepod dominating the mesozooplankton biomass in the NWA (Plank et al. 1997). Broad-scale trend showed an increase in mean *C. finmarchicus* abundance at the beginning of the 2000s, followed by a general decline from approximately 2005 to 2015 with the exception of the high abundance values of 2010 (Fig. 9A). Mean annual abundance increased almost steadily after the record-low level of 2015, and reached the second highest value of the time series in 2021 (Fig. 9A). The abundance of *Calanus finmarchicus* showed a general decrease in 2022 compared to the previous year, especially on Seal Island (2J) and Bonavista (3K) sections where abundances dropped from above normal to near normal and below normal, respectively (Fig. 10A). The decline of *C. finmarchicus* copepods on these two sections may be partly attributable to the missing summer survey since *C. finmarchicus* abundance is generally maximum between June and August in that region. *C. finmarchicus* abundance was near normal in the Gulf of St. Lawrence in 2022 and did not depart strongly from the conditions observed in the previous year except for the Rimouski station (4T) where abundance dropped from above normal in 2021 to below normal in 2022 (Fig. 10A). The abundance pattern of *C. finmarchicus* on the Scotian Shelf in 2022 was also similar to that of the previous year with near-to-below-normal levels across the region (Fig. 10A).

*Pseudocalanus* spp. are highly abundant small copepod taxa that are widely distributed across the NWA (Pepin et al. 2011). They are important prey items for of ecologically important fish species such as herring and capelin (Möllmann et al. 2004, Murphy et al. 2018, Wilson et al. 2018,) and their abundance generally covary with that of other numerically abundant small copepod taxa in the NWA. Mean abundance of *Pseudocalanus* spp. copepods was mostly near normal throughout the 2000s (Fig. 9B). Abundance increased during the early 2010s up to a record high in 2015, and slowly declined afterward to reach its lowest level in 10 years in 2022 (Fig. 9B). On the Newfoundland Shelf, the abundance of *Pseudocalanus* spp. copepods increased from near normal to above normal on the Seal Island section (2J) in 2022 compared to the previous year, but it markedly decreased from above normal to below normal along the Bonavista section (3K) during the same period (Fig. 10B). On the Grand Bank, *Pseudocalanus* spp. abundance decreased from above normal to near normal on the northern Grand Bank (3L portion of the Flemish Cap section), and remained respectively above and below normal at Station 27 (3L) and on the Flemish Cap (3M part of the Flemish Cap section) (Fig. 10B). The abundance pattern of *Pseudocalanus* spp. in the Gulf of St. Lawrence remained similar to that of the previous with above-normal levels on the eastern GSL section (4RS) and at the Rimouski and Shediak stations (4T), below-normal levels in the northeast (4ST) and central (4RST) GSL, and a near-normal level in the Cabot Strait (3Pn, 4Vn) (Fig. 10B). On the Scotian Shelf, *Pseudocalanus* spp. abundance was near normal everywhere in 2022 except for the above-normal level observed at the Prince 5 station in the Bay of Fundy (Fig. 10B). Compared to the previous year, this represented an increase for the Louisbourg section (4Vs), a decrease for the Halifax (4W) and the Browns Bank (4X) sections, and the status quo for the Halifax 2 station (4W) (Fig. 10B).

Mean zooplankton biomass showed a similar temporal variation pattern than that of *C. finmarchicus* with an increase in the early 2000s followed by a general decline through to a minimum low in 2015, and mostly near normal levels afterwards with the exception of the high biomass values observed in 2021 (Fig. 11). In 2022, zooplankton biomass declined almost everywhere on the Newfoundland Shelf and the Grand Bank compared



to the previous year but still remained above normal on the Seal Island (2J) section and the northern Grand Bank (3L portion of the Flemish Cap section), while decreasing from above normal to near normal along the Bonavista section and the Flemish Cap (3M portion of the Flemish Cap section) (Fig. 12). Part of this decrease may be attributable to the missing summer survey in Newfoundland Region since zooplankton biomass is generally maximum in summer. Zooplankton biomass was markedly low on the eastern GSL (4RS) and at the Rimouski station (4T) but increased from near normal to above normal in the southern GSL and at the Shediac Valley station (4T) (Fig. 12). On the Scotian Shelf, zooplankton biomass was below normal everywhere except at the Prince 5 station (4X) in the Bay of Fundy where biomass had remained above normal for a second consecutive year (Fig. 12).

#### 4. Relationships between ocean climate and biogeochemical oceanographic conditions

Not surprisingly, the correlation matrix (Fig. 13) indicated significant correlations between the composite NL climate index and each of its selected subcomponents, i.e., winter NAO, air temperature, sea ice cover, sea surface temperature (SST), and bottom temperature. Several of the NL climate index subcomponents were also significantly correlated among each other. The positive phase of the winter NAO index is associated with colder climatic conditions in the Newfoundland and Labrador region and, conversely, its negative phase is associated with warmer climate (Colbourne et al. 1994) which aligns with the significant positive relationship between the winter NAO and sea ice cover. All other correlations among the climate index subcomponents were as expected, e.g., air temperature positively correlated with SST and bottom temperature, and negatively correlated with sea ice cover.

More interesting were the relationships between ocean climate and some of the biological indices. The initiation of the spring phytoplankton bloom was negatively correlated with the NL climate index, air temperature and sea bottom temperature, and positively correlated with the winter NAO index and sea ice cover. This indicates that warmer conditions are favourable to earlier spring blooms, mainly because of a reduction in the sea ice cover and an earlier onset of water column vertical stratification (Chiswell 2011, Rumyantseva et al. 2019). Interestingly, the expected negative correlation between initiation and SST was not significant. The significant negative correlation between spring bloom initiation and duration indicates that early bloom last longer and suggests that bloom duration is primarily controlled by the onset timing of the bloom. The correspondence between remote sensing and *in situ* measurement of chlorophyll *a* was confirmed by the positive correlations between bloom duration and magnitude indices derived from satellite observations, and depth-integrated inventories (chl *a* 0-100 m) measured during seasonal oceanographic surveys.

Zooplankton play a critical role in the oceanic food chain and represent one of the main mechanisms of energy transfer from primary production to higher trophic levels. Their abundance and distribution in marine ecosystems directly or indirectly impact the state of several ecologically and economically important stocks from forage fish to whales (Pendleton et al. 2009, Plourde et al. 2019). In the NWA, both the abundance and biomass of zooplankton are dominated by copepods but other non-copepod organisms such as euphausiids, amphipods, pteropods, larvaceans, and chaetognaths are also of significant ecological importance. Total copepod abundance is mainly driven by small copepod taxa (Pepin et al. 2011) as highlighted by the significant positive correlation between total copepod abundance and the abundance of small *Pseudocalanus* spp. copepods. Other small copepod taxa such as *Oithona* spp. and *Temora longicornis* are also numerically dominant and their abundance generally covary with that of *Pseudocalanus* spp. but also with that of other small planktonic organisms such as appendicularians and bivalve larvae that dominate the abundance of non-copepod zooplankton (Maillet et al. 2022). Bottom-up factors such as variability in phytoplankton community composition and size structure likely have similar impacts on small copepod and non-copepod organisms but more research is needed to clearly identify the drivers of abundance of these taxa. Zooplankton biomass is also dominated by copepods and is primarily controlled by the large *C. finmarchicus* which, in the North Atlantic, generally accounts for more than half of the total zooplankton biomass despite their comparatively lower abundance (Planque & Batten 2000, Head et al. 2003). This is confirmed by the significant positive correlations between zooplankton biomass and total both total copepod and *C. finmarchicus* abundance.

*C. finmarchicus* are primarily herbivore copepods with an annual life cycle. Subadults of *C. finmarchicus* emerge from dormancy in early spring and migrate toward the surface before the initiation of the spring phytoplankton bloom to moult and mate. Females release their eggs into near surface waters where individuals hatch and develop until the end of the summer when they return to depth to overwinter (Head & Pepin 2008, Melle et al. 2014, Head et al. 2013). Egg production in *C. finmarchicus* females is positively related to phytoplankton biomass in the North Atlantic (Jónasdóttir et al. 2002) and the significant correlation between *C. finmarchicus* abundance and the NL climate index (+), winter NAO (-), sea ice cover (-) and spring bloom initiation (-) suggest that early spring blooms associated with warmer environmental conditions are favourable to *C. finmarchicus* reproduction success and offspring survival.

## 5. Biogeochemical oceanographic highlights for 2022

- The initiation of the spring phytoplankton bloom was, on average, earlier than normal in the Gulf of St. Lawrence and on the Scotian Shelf, later than normal on the Grand Bank and the Flemish Cap, and near normal elsewhere.
- Bloom duration was either near normal or slightly shorter than normal across the region in 2022.
- The magnitude of the spring phytoplankton bloom was, on average, below normal on the Grand Bank, above normal on the southern Newfoundland and the Scotian Shelf, and near normal elsewhere.
- Mean nitrate inventories increased to above-normal in 2022 for the first time since 2015.
- Mean chlorophyll inventories remained near normal for a 2<sup>nd</sup> consecutive year in 2022 after two consecutive years of above-normal levels.
- Total copepod abundance decreased to near normal after two consecutive years of above-normal levels. Copepod abundance in 2022 was at its lowest level in 20 years and was particularly low on the Flemish Cap and in southern Newfoundland.
- The abundances of *Calanus finmarchicus* and *Pseudocalanus* spp. copepods were near normal but at their lowest levels since 2015 and 2012, respectively.
- Mean total zooplankton biomass for the region decreased from above normal to near normal in 2022 and was at its second lowest level since 2015.

## Acknowledgments

We thank the personnel at the Northwest Atlantic Fisheries Center (NL Region), the Bedford Institute of Oceanography and (Maritimes Region), the Maurice -Lamontagne Institute (Quebec Region), the St. Andrews Biological Station and various offices in the Gulf Region who contributed to sample collection, sample analysis, data analysis, data management, and data sharing. We also thank the officers and crews of the Canadian Coast Guard Ships and other research vessels who assisted with the collection of oceanographic data during 2022.

## References

- Blais M, Galbraith PS, Plourde S, Devred E, Clay S, Lehoux C and Devine L (2021) Chemical and biological oceanographic conditions in the Estuary and Gulf of St. Lawrence during 2020. DFO Can. Sci. Advis. Sec. Res. Doc. 2021/060. iv + 67 p.
- Bristow LA, Mohr W, Ahmerkamp S and Kuypers MM (2017) Nutrients that limit growth in the ocean. Curr 27: R431-R510
- Casault B, Johnson C, Devred E, Head E and Beazley L (2023). Optical, chemical, and biological oceanographic conditions on the Scotian Shelf and in the eastern Gulf of Maine in 2021. DFO Can. Sci. Advis. Sec. Res. Doc. 2023/016. v + 74 p.
- Chiswell SM (2011) Annual cycles and spring blooms in phytoplankton: don't abandon Sverdrup completely. Mar Ecol Prog Ser 443:39-50
- Clay S, Layton C and Devred E (2021) BIO-RSG/PhytoFit: First release (v1.0.0). Zenodo. <https://doi.org/10.5281/zenodo.4770754>.
- Colbourne E, Narayanan S and Prinsenberg S (1994) Climatic changes and environmental conditions in the Northwest Atlantic, 1970-1993. ICES J of Mar Sci Symp 198: 311-322
- Cyr F, Snook S, Bishop C, Bishop C, Galbraith PS, Chen N, Han G (2022) Physical oceanographic conditions on the Newfoundland and Labrador Shelf during 2021. DFO Can. Sci. Advis. Sec. Res. Doc. 2022/040 iv + 48 p.
- Cyr F and Galbraith PS (2021) A climate index for the Newfoundland and Labrador Shelf. Earth Syst Sci Data 13: 1807-1828
- Galbraith PS, Chassé J, Dumas J, Shaw J-L, Caverhill C, Lefavre C and Lafleur C (2021) Physical oceanographic conditions in the Gulf of St. Lawrence during 2021. DFO Can. Sci. Advis. Sec. Res. Doc. 2022/034. iv + 83 p.
- Head EJH, Harris LR and Yashayaev I (2003) Distributions of *Calanus* spp. and other mesozooplankton in the Labrador Sea in relation to hydrography in spring and summer (1995-2000). Prog Oceanogr 59: 1-30.
- Head EJH and Pepin P (2008) Variations in overwintering depth distributions of *Calanus finmarchicus* in the slope waters of the NW Atlantic continental shelf and the Labrador Sea. J Northwest Atl Fish Sci 39: 49-69.
- Head EHJ, Melle W, Pepin P, Bagøien E and Broms C (2013) On the ecology of *Calanus finmarchicus* in the Subarctic North Atlantic: A comparison of population dynamics and environmental conditions in areas of the Labrador Sea-Labrador/Newfoundland Shelf and Norwegian Sea Atlantic and Coastal Waters. Prog Oceanogr 114, 46-63.

- Hebert D, Layton C, Brickman D, and Galbraith PS (2021) Physical oceanographic conditions on the Scotian Shelf and in the Gulf of Maine during 2020. DFO Can. Sci. Advis. Sec. Res. Doc. 2021/070. v + 55 p.
- Jónasdóttir SH, Gudfinnsson HG, Gislason A, Astthorsson OS (2002) Diet composition and quality for *Calanus finmarchicus* egg production and hatching success off south-west Iceland. Mar Biol 140: 1195-1206
- Koen-Alonso M, Pepin P, Fogarty M, Kenny A nd Kenchington E (2019) The Northwest Atlantic Fisheries Organization Roadmap for the development and implementation of an Ecosystem Approach to Fisheries: structure, state of development, and challenges. Mar Policy 100: 342-352
- Maillet G, Bélanger D, Doyle G, Robar A, Rastin S, Ramsay D and Pepin P (2022) Optical, chemical and biological oceanographic conditions on the Newfoundland and Labrador Shelf during 2018. DFO Can. Sci. Advis. Sec. Res. Doc. 2022/075. Viii + 53 p.
- Melle W, Runge F, Head E, Plurde S, and others (2014) The North Atlantic Ocean as habitat for *Calanus finmarchicus*: Environmental factors and life history traits. Prog Oceanogr 129: 244-284
- Mitchell MR, Harrison G, Pauley K, Gagné A, Maillet G and Strain P (2002) Atlantic Zone Monitoring Program Sampling Protocol. Canadian Technical Report of Hydrography and Ocean Sciences 223, 23 pp.
- Möllmann C, Kornilovs G, Fetter M and Köster FW (2004) Feeding ecology of central Baltic Sea herring and sprat. J Fish Biol 65:1563-1581
- Murphy HM, Pepin P, and Robert D (2018) Re-visiting the drivers of capelin recruitment in Newfoundland since 1991. Fish Res 200: 1-10
- Pendleton DE, Pershing AJ, Brown MW, Mayo CA, Kenedy, RD, Record NR, Cole TVN (2009) Regional-scale mean copepod concentration indicates relative abundance of North Atlantic right whales. Mar Ecol Prog Ser 378: 211-225
- Pepin P, Colbourne E, Maillet G (2011) Seasonal patterns in zooplankton community structure on the Newfoundland and Labrador Shelf. Prog Oceanogr 91: 273-285
- Plank B, Hays GC, Ibanez F, Gamble JC (1997) Large scale variations in the seasonal abundance of *Calanus finmarchicus*. Deep-Sea Res 44: 315-326
- Planque B and Batten DS (2000) *Calanus finmarchicus* in the North Atlantic: the year of *Calanus* in the context of interdecadal change. ICES J Mar Sci 57: 1528-1535.
- Plourde S, Lehoux C, Johnson CL and Lesage V (2019) North Atlantic right whale (*Eubalaena glacialis*) and its food: (I) a spatial climatology of *Calanus* biomass and potential foraging habitats in Canadian waters. J Plankton Res 41: 667-685
- Ringuette M, Devred E, Azetsu-Scott K, Head E, Punshon S, Casault B and Clay S (2022). Optical, chemical, and biological oceanographic conditions in the Labrador Sea between 2014 and 2018. DFO Can Sci Advis Sec Res Doc 2022/021. V + 38 p.
- Rumyantseva A, Henson S, Martin A, Thompson AF, Damerell GM, Kaiser J, Heywood KJ (2019) Phytoplankton spring bloom initiation: The impact of atmospheric forcing and light in the temperate North Atlantic Ocean. Prog Oceanogr 178: 102202
- Yashayaev I, Peterson I and Wang Z (2021). Meteorological, sea ice, and physical oceanographic conditions in the Labrador Sea during 2019. DFO Can. Sci. Advis. Sec. Res. Doc. 2021/074. iv +38 p.

Zhai L, Platt T, Tang C, Sathyendranath S, Walls, RH (2011) Phytoplankton phenology on the Scotian Shelf.  
ICES J Mar Sci 68: 781-791

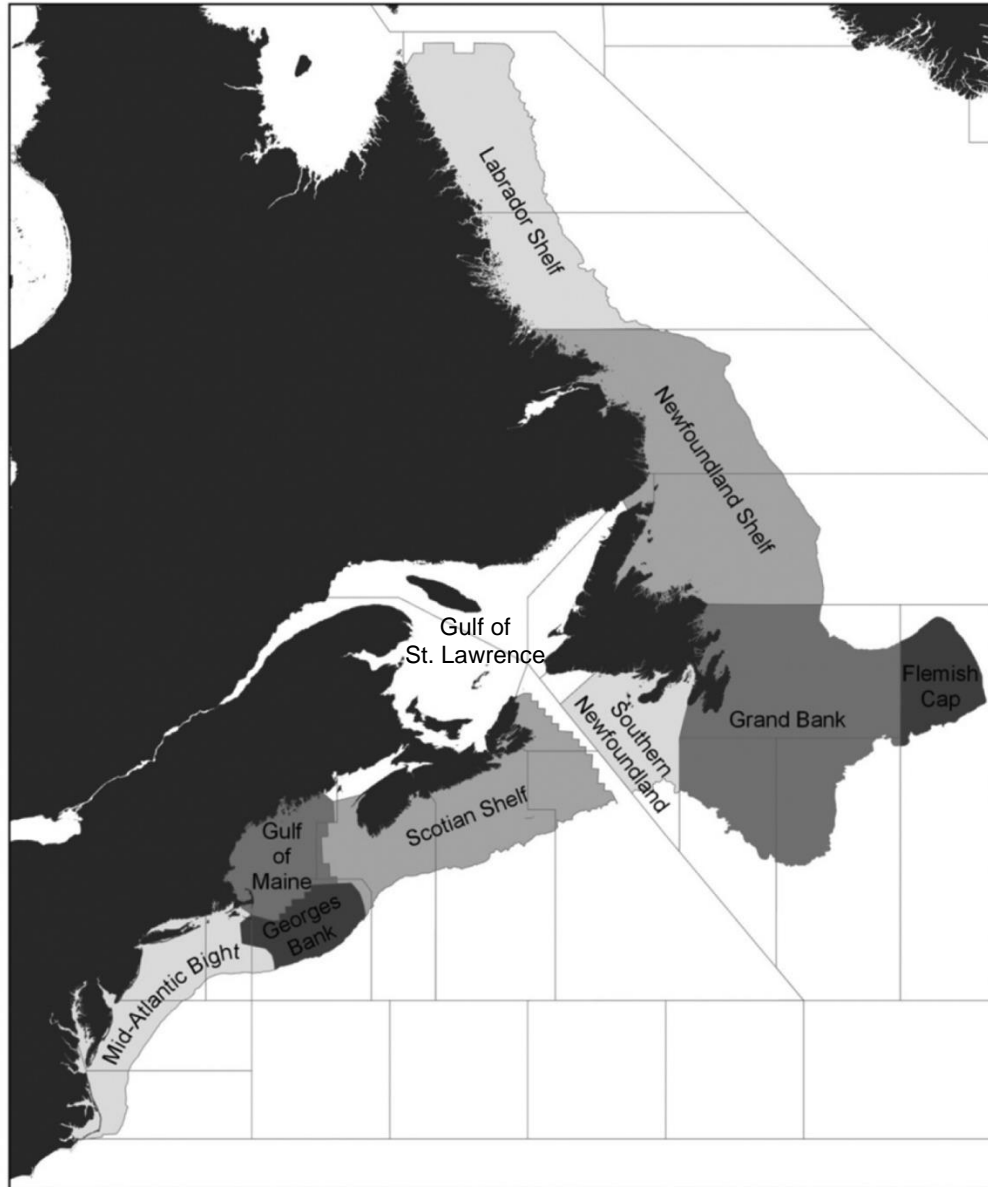


**Figure 1.** NAFO Ecological Production Units (EPUs) used to summarize biogeochemical oceanographic conditions in the NW Atlantic. The Gulf of St. Lawrence is also used as a grouping unit although it is not an official EPU. This report does not address conditions in the Gulf of Maine, and Mid-Atlantic Bight EPUs. Figure modified from Koen-Alonso et al. 2019.

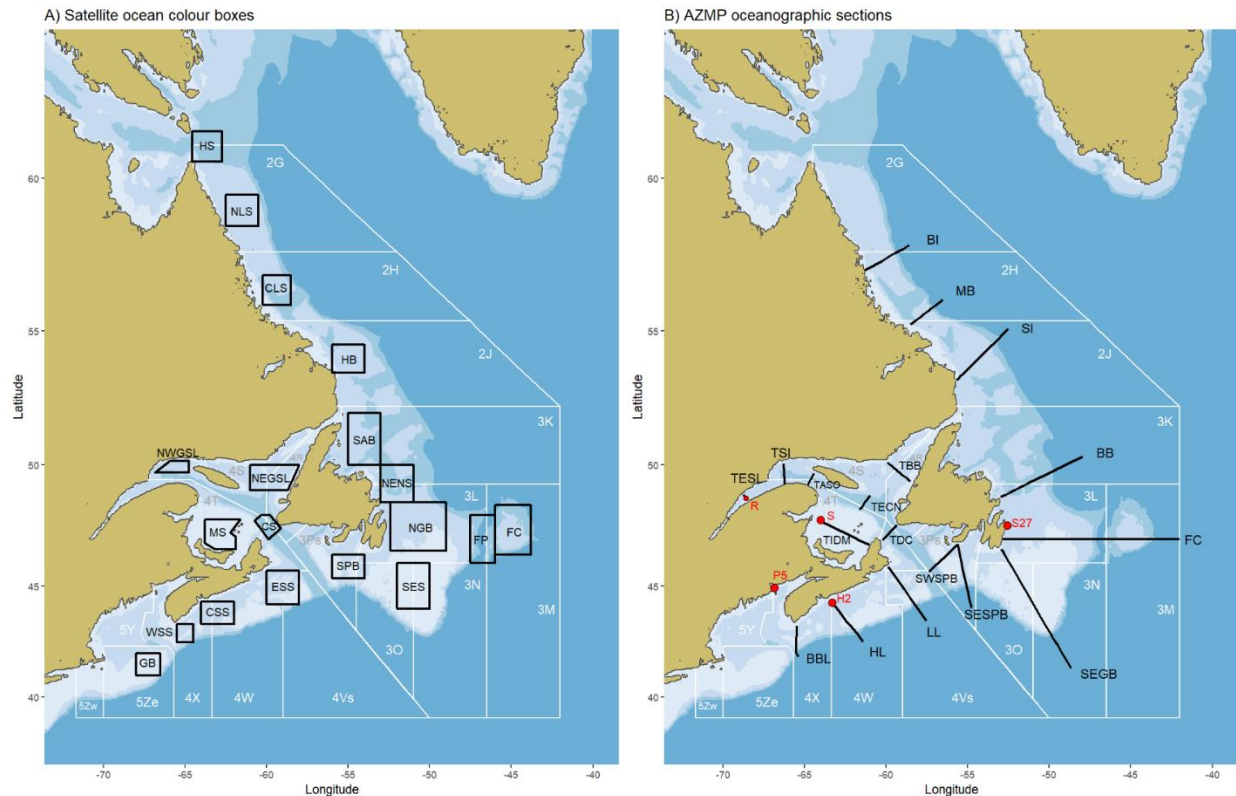


**Figure 2.** (A) Location of the boxes used to calculate spring bloom indices (initiation duration, magnitude) from satellite Ocean Color imagery: (HS=Hudson Strait, NLS=northern Labrador Shelf, CLS=central Labrador Shelf, HB=Hamilton Bank, SAB=St. Anthony Basin, NENS=northeast Newfoundland Shelf, FP=Flemish Pass, FC=Flemish Cap, NGB=northern Grand Bank, SES=southeast Shoal, SPB=Green-St. Pierre Bank, NEGSL=northeast Gulf of St. Lawrence, NWGSL=northwest Gulf of St. Lawrence, MS=Magdalen Shallows, ESS=eastern Scotian Shelf, CSS=central Scotian Shelf, WSS=western Scotian Shelf. (B) Location of Atlantic Zone Monitoring Program (AZMP) oceanographic sections (black lines: BI=Beachy Island; MB=Makkovik Bank; SI=Seal Island; BB=Bonavista Bay; FC=Flemish Cap; SEGB=Southeastern Grand Bank; TBB+TCEN+TDC=Eastern Gulf of St. Lawrence; TESL+TSI+TASO=Western Gulf of St. Lawrence; TIDM=Southern Gulf of St. Lawrence; LL=Louisbourg Line; HL=Halifax Line; BBL=Brown Bank Line), and coastal high-frequency monitoring sites (red circles: S27=Station 27; R=Rimouski; S=Shediac Valley; H2=Halifax 2; P5=Prince 5) where biogeochemical data (nitrate, chlorophyll *a*, zooplankton abundance and biomass) were collected.

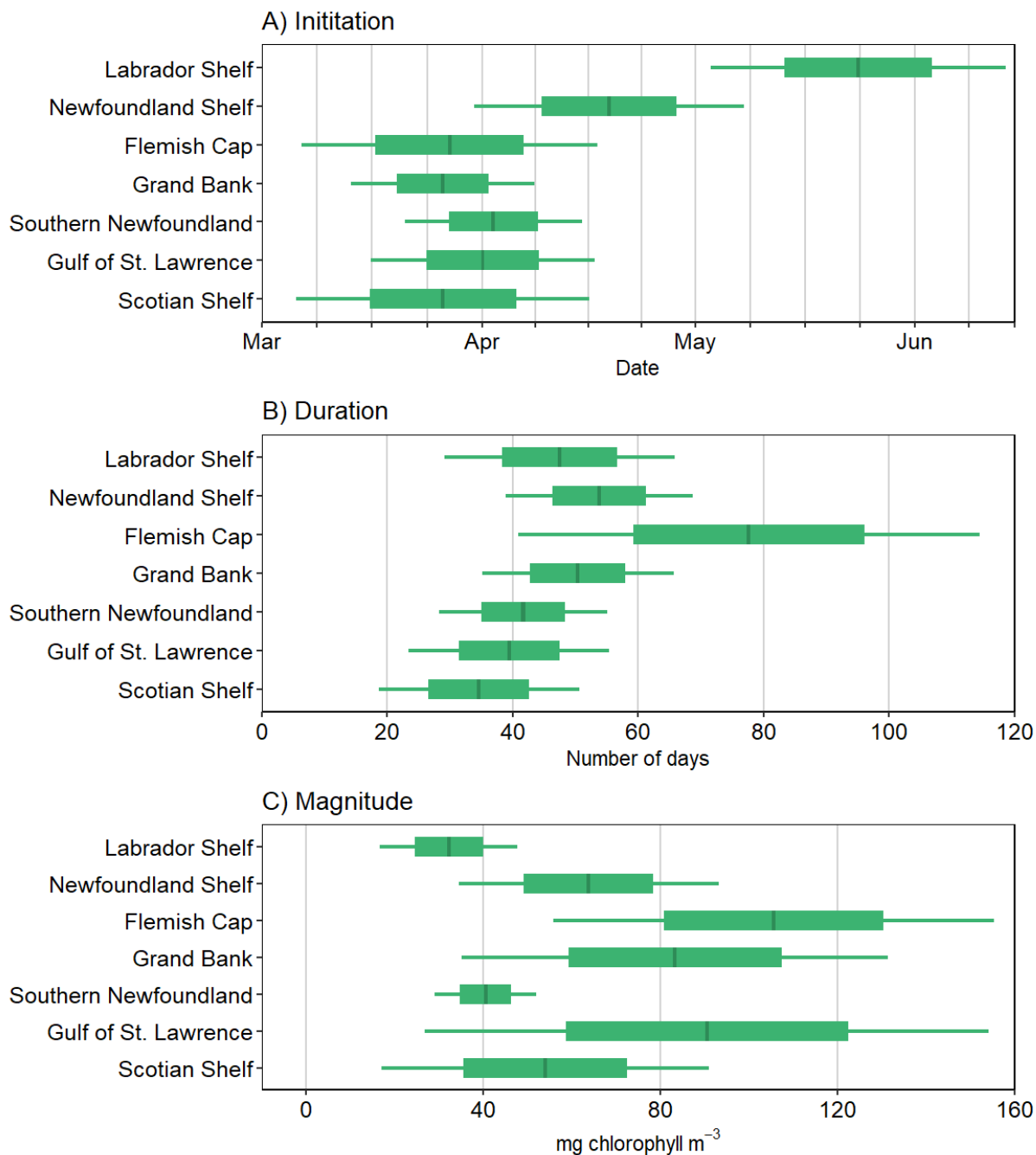


**Figure 3.** Mean values  $\pm 0.5$  SD (rectangles) and  $\pm 1$  SD (whiskers) for the spring phytoplankton bloom (A) initiation, (B) duration, and (C) magnitude derived from ocean colour satellite data over the 2003-2020 reference period. The three parameters were calculated for six NAFO Ecological Production Units (EPUs: Labrador Shelf, Newfoundland Shelf, Flemish Cap, Grand Bank, Southern Newfoundland, Scotian Shelf) and for the Gulf of St. Lawrence. See Fig. 1 for EPUs locations.



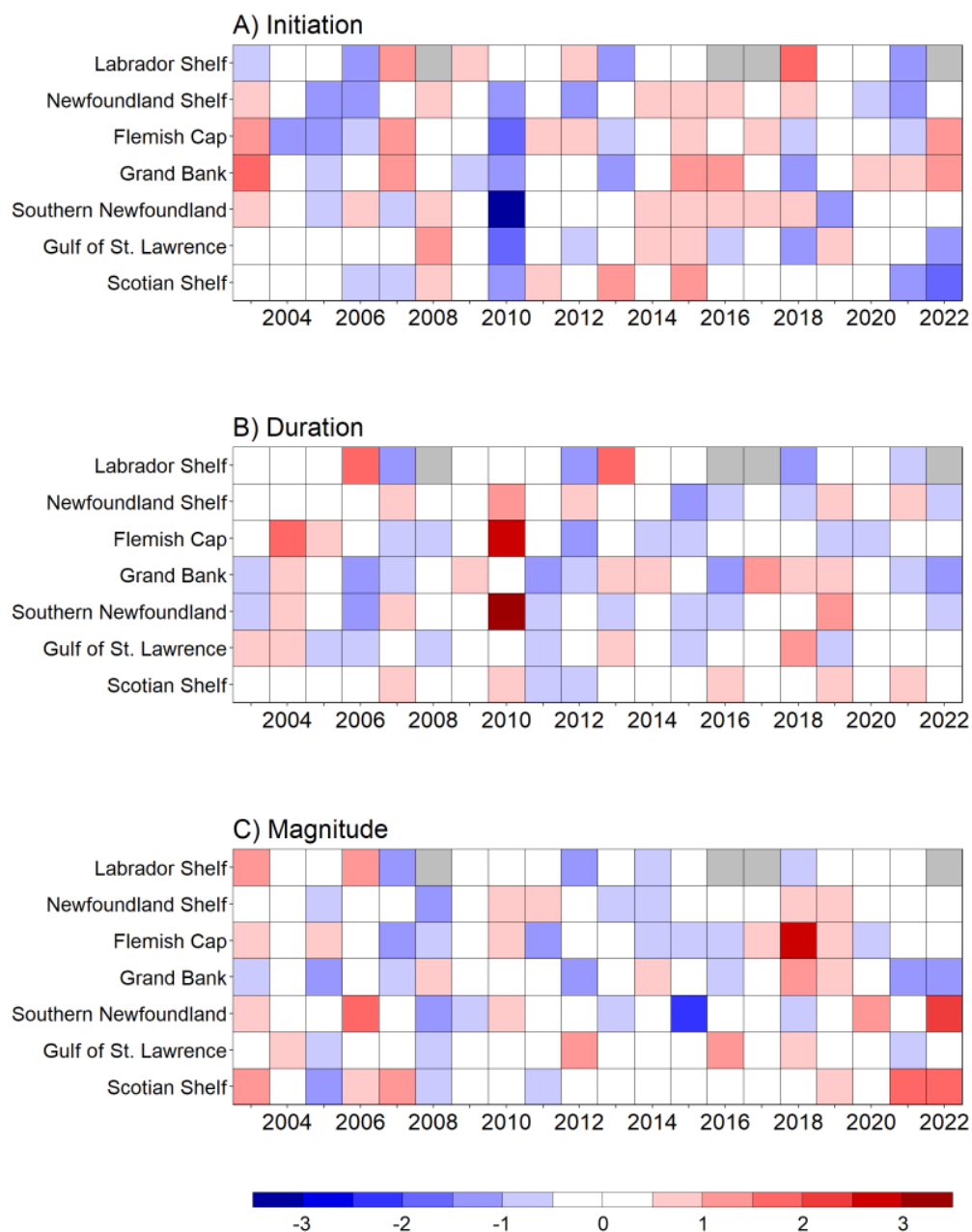


**Figure 4.** Annual standardized anomaly scorecards for the spring phytoplankton bloom (A) initiation, (B) duration, and (C) magnitude for seven NAFO Ecological Production Units (EPU) and for the Gulf of St. Lawrence (GSL). Standardized anomalies were calculated for each oceanographic section and high-frequency monitoring site using a 2003-2020 reference period and averaged over geographical grouping units (EPUs or GSL). Red (blue) cells indicate later (earlier) bloom initiation, longer (shorter) bloom duration, or higher (lower) bloom magnitude relative to the 2003-2020 reference period. White cells indicate near-normal conditions, i.e.  $\pm 0.5$  SD from the mean for the reference period. Grey cells indicate years for which limited data availability did not permit index calculation. Regions are listed from North (top) to south (bottom). See Fig. 1 for the location of geographical grouping units.

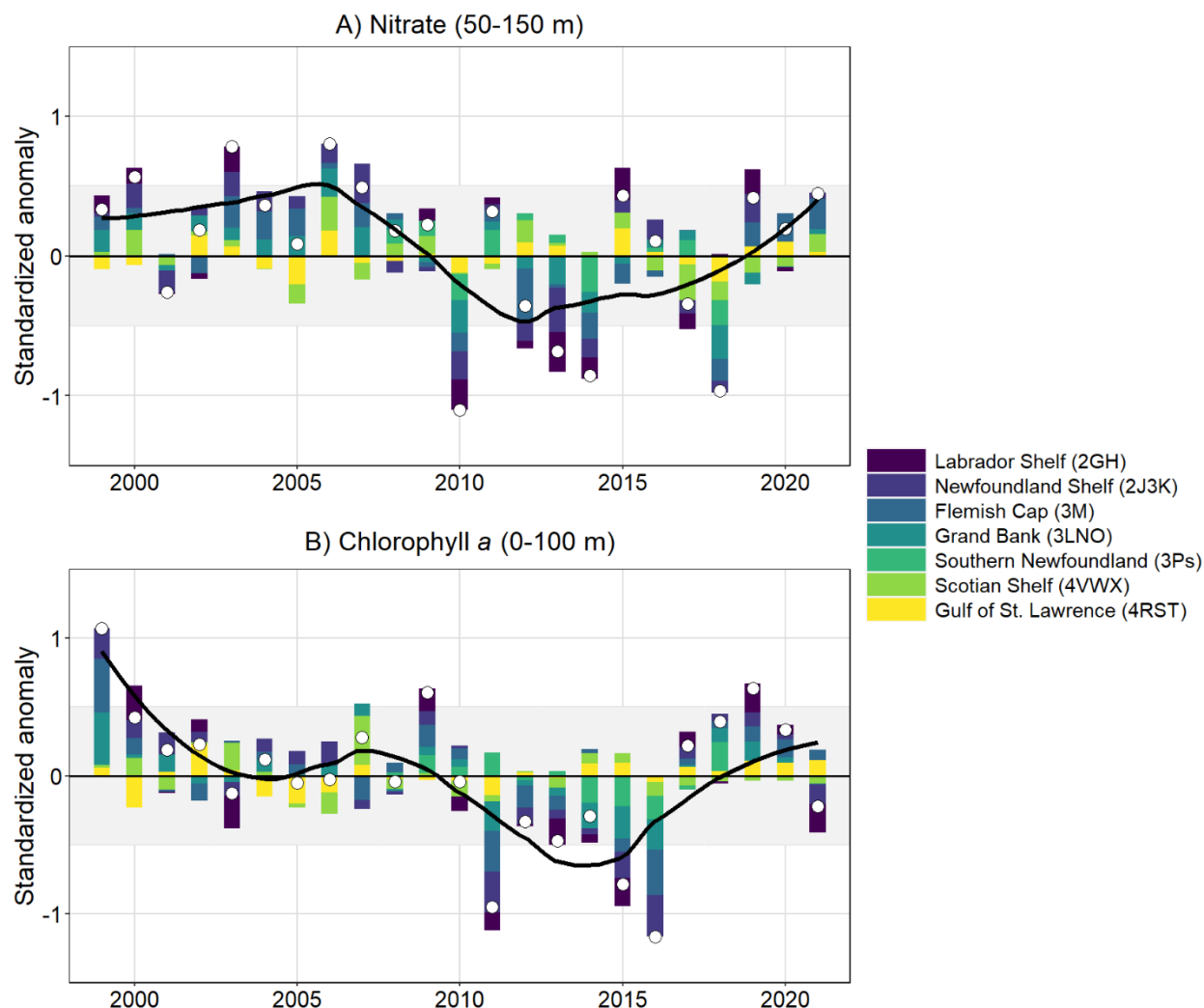


**Figure 5.** Annual anomaly time series of (A) 50-150 m integrated nitrate, and (B) 0-100 m integrated chlorophyll-*a* inventories in six NAFO Ecological Production Units (EPU) and in the Gulf of St. Lawrence (GSL). Standardized anomalies were calculated for each oceanographic section and high-frequency monitoring site using a 1999-2020 reference period and averaged over geographical grouping units (EPUs or GSL). White circle indicate the mean annual anomaly for the Northwest Atlantic (NWA). Colour bars indicate the relative contribution of each grouping unit to the mean anomaly. The black line is a loess regression fitted to the annual mean anomalies that summarizes the broad-scale temporal trend observed across the NWA. See Figs. 1 & 2B for the location of geographical grouping units, oceanographic sections and high-frequency monitoring sites.

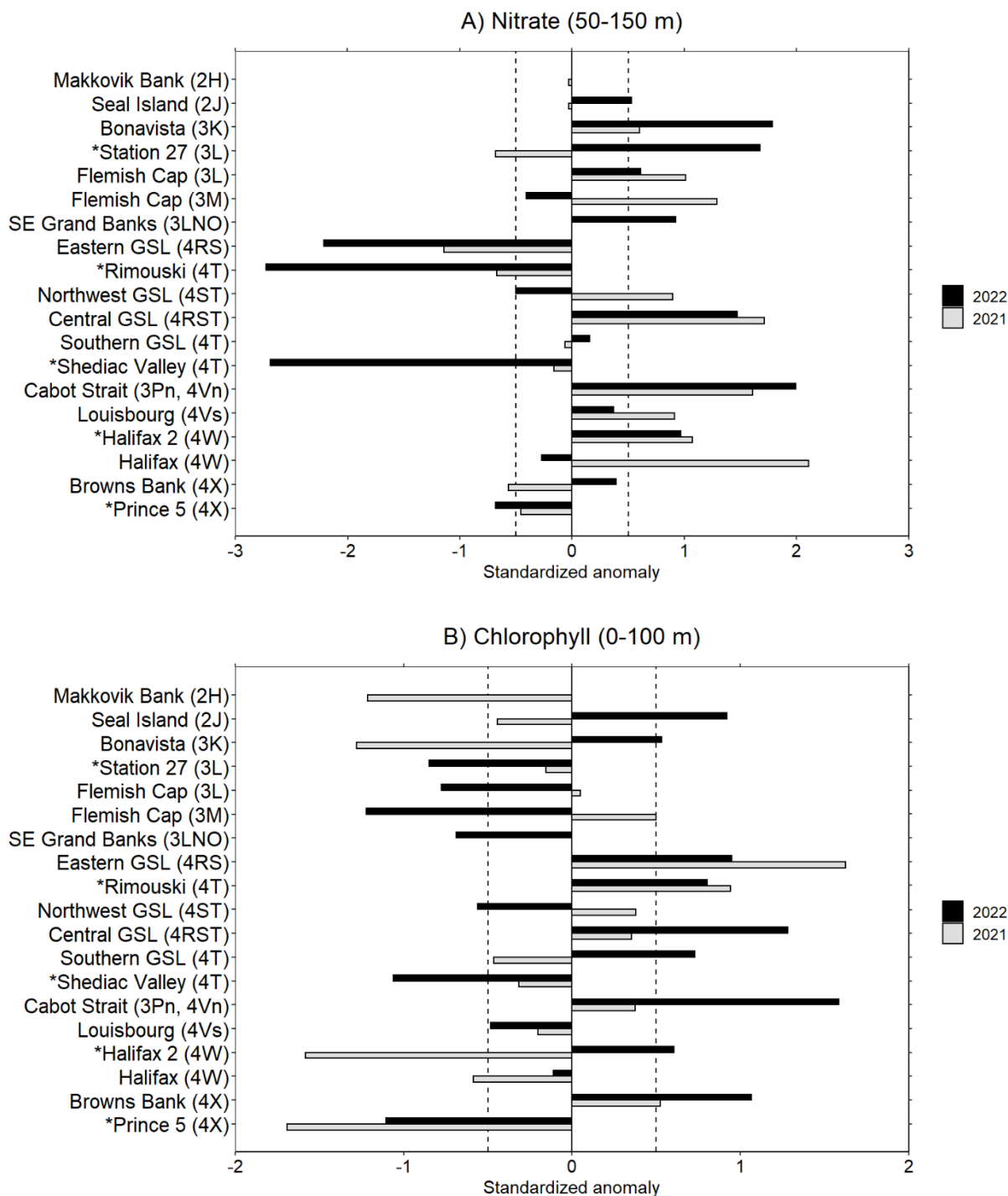


**Figure 6.** Comparison between 2021 and 2022 annual anomalies of (A) 50-150 integrated nitrate, and (B) 0-100 m integrated chlorophyll-*a* inventories for each AZMP oceanographic section and high-frequency monitoring site sampled by the AZMP. Anomalies were calculated based on a 1999-2020 reference period. Anomalies within  $\pm 0.5$  SD (vertical dashed lines) are considered to represent near-normal conditions. Sampling locations are listed from north (top) to south (bottom). Asterisks (\*) indicate high-frequency monitoring sites. See Figure 2B for oceanographic sections and high-frequency monitoring sites location.

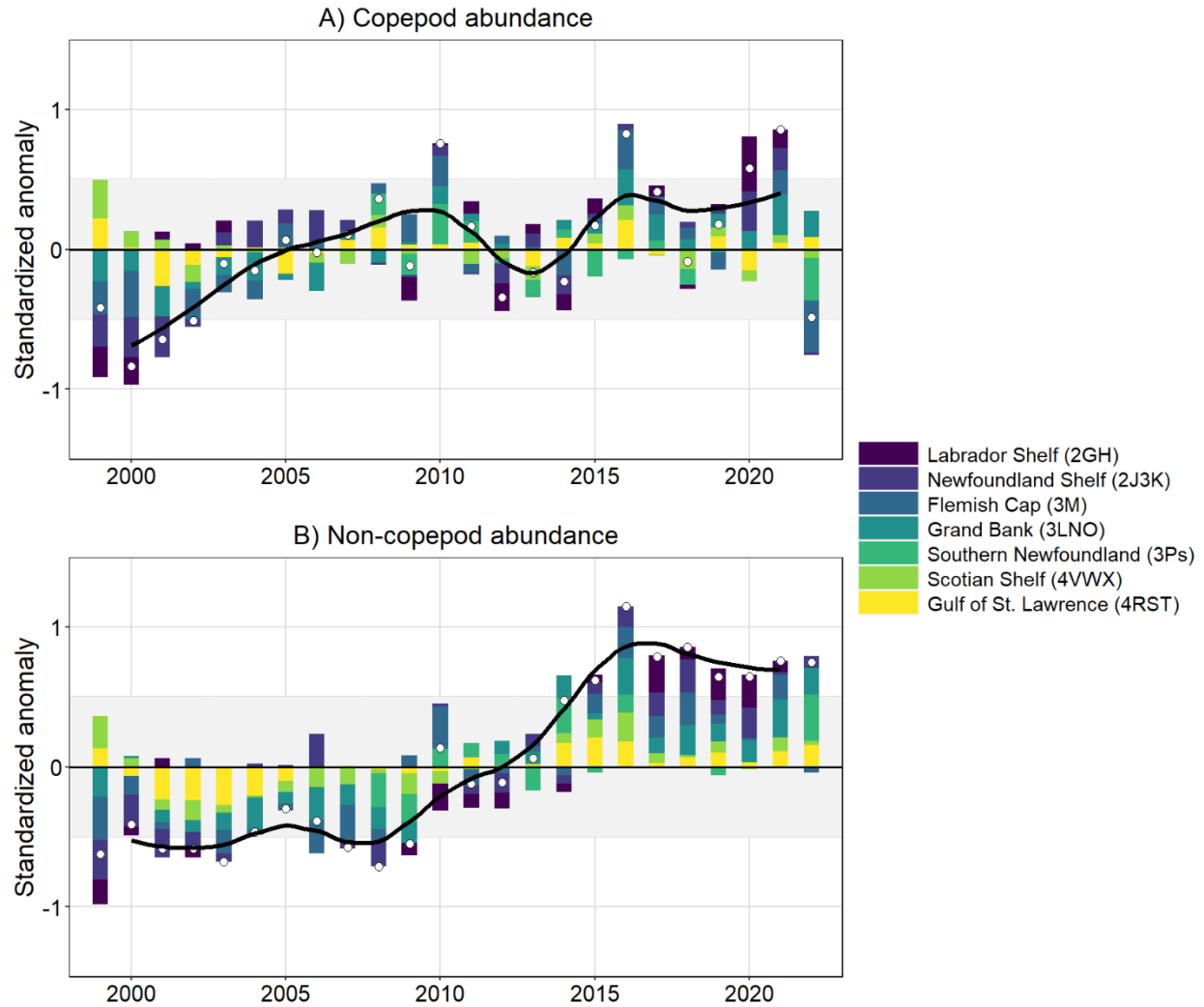


**Figure 7.** Anomaly time series of (A) copepod, and (B) non-copepod zooplankton abundance ( $\text{ind.} \cdot \text{m}^{-2}$ ) in six NAFO Ecological Production Units (EPU) and in the Gulf of St. Lawrence (GSL). Standardized anomalies were calculated for each oceanographic section and high-frequency monitoring site using a 1999-2020 reference period and averaged over geographical grouping units (EPUs or GSL). White circle indicate the mean annual anomaly for the Northwest Atlantic (NWA). Colour bars indicate the relative contribution of each grouping unit to the mean anomaly. The black line indicate the overall trend across the NWA based on 3-y running average of annual mean anomalies. See Figs. 1 & 2B for the location of geographical grouping units, oceanographic sections and high-frequency monitoring sites.

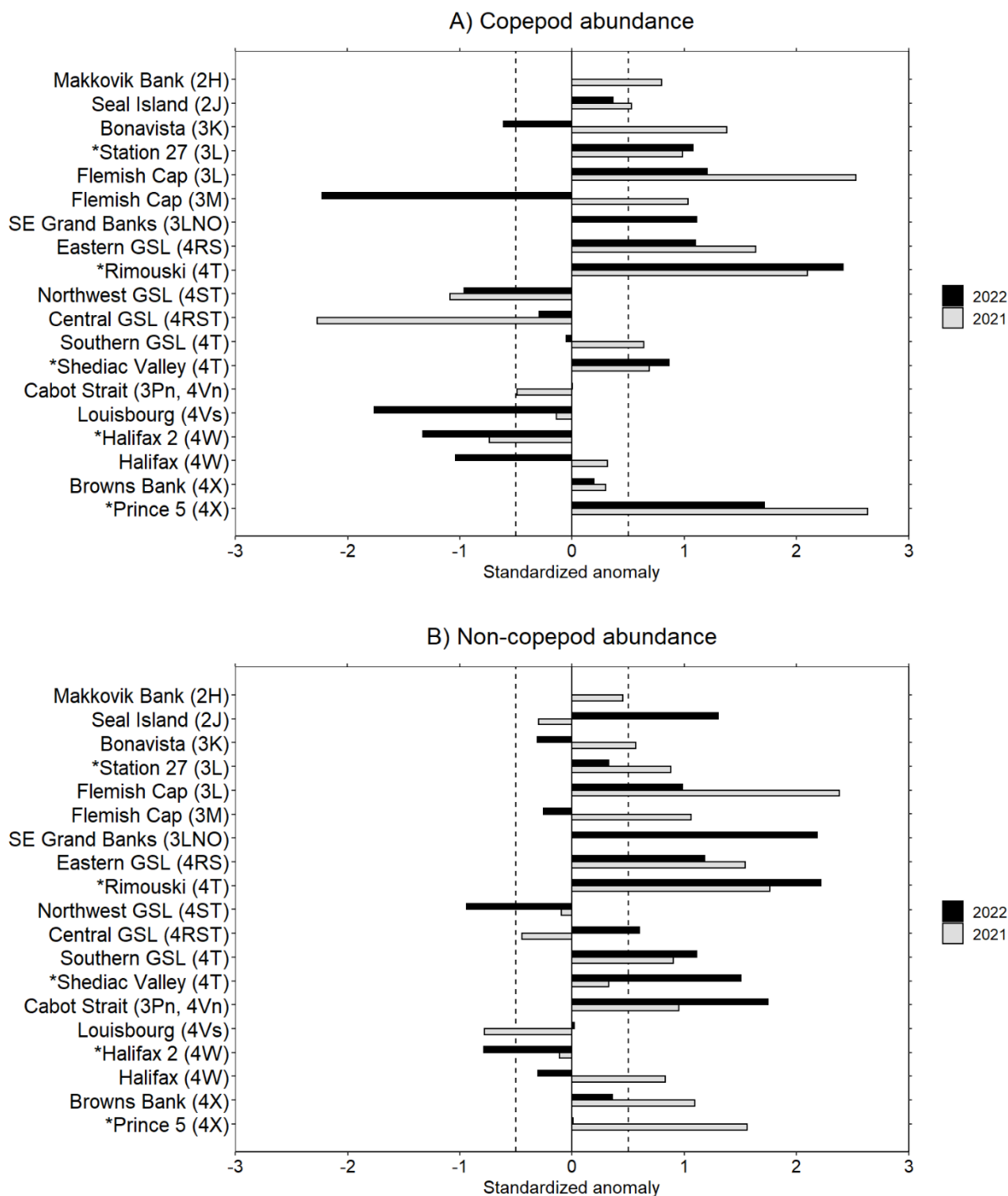


**Figure 8.** Comparison between 2021 and 2022 annual anomalies for copepod (A), and non-copepod (B) abundance ( $\text{ind.} \cdot \text{m}^{-2}$ ) for each AZMP oceanographic section and high-frequency monitoring site sampled by the AZMP. Anomalies are calculated based on a 1999-2020 reference period. Anomalies were calculated based on a 1999-2020 reference period. Anomalies within  $\pm 0.5$  SD (vertical dashed lines) are considered to represent near-normal conditions. Sampling locations are listed from north (top) to south (bottom). Asterisks (\*) indicate high-frequency monitoring sites. See Figure 2B for oceanographic sections and high-frequency monitoring sites location.

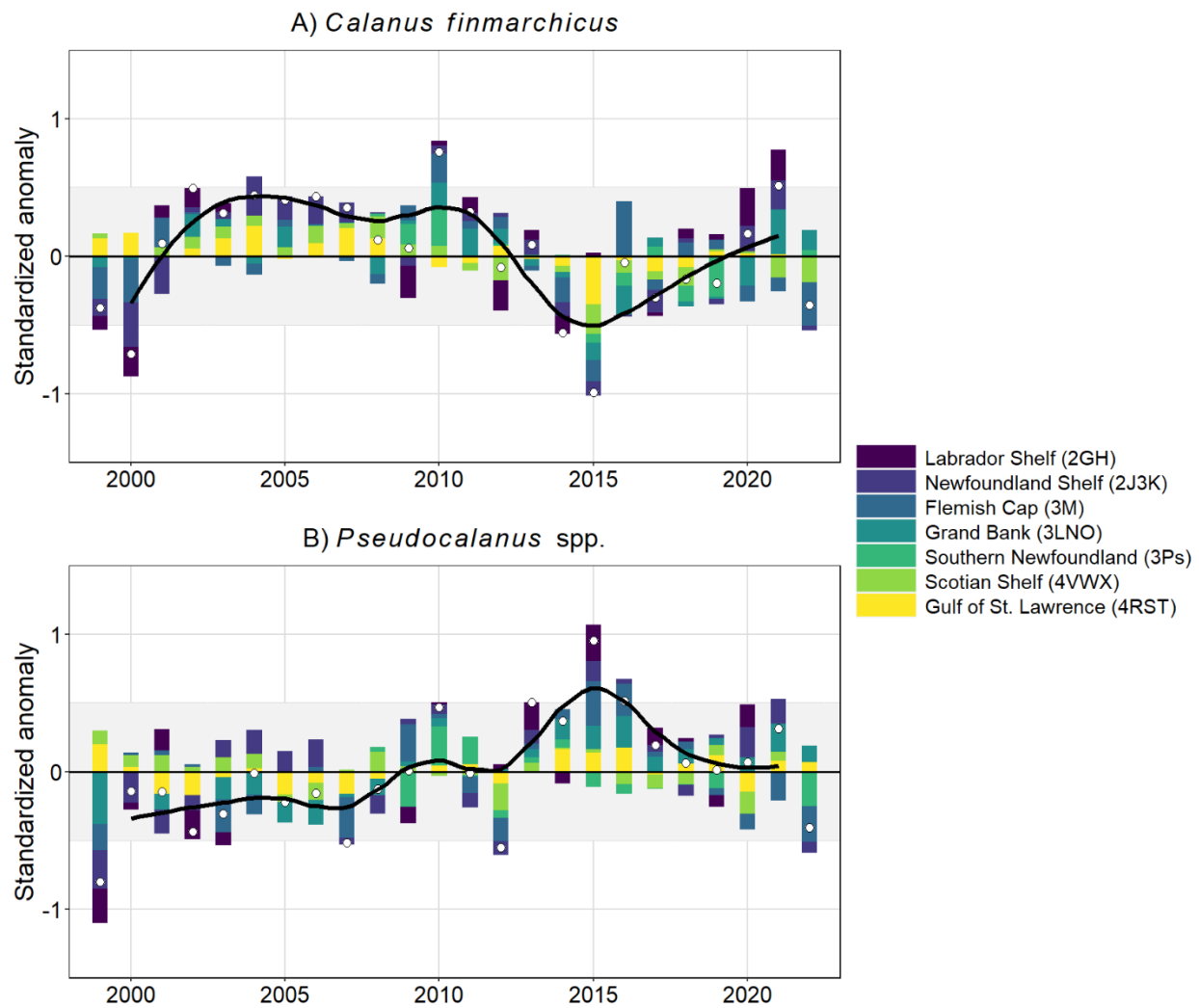


**Figure 9.** Annual anomaly time series of (A) *Calanus finmarchicus* and (B) *Pseudocalanus* spp. copepod abundance (ind. m<sup>-2</sup>) in six NAFO Ecological Production Units (EPU) and in the Gulf of St. Lawrence (GSL). Standardized anomalies were calculated for each oceanographic section and high-frequency monitoring site using a 1999-2020 reference period and averaged over geographical grouping units (EPUs or GSL). White circle indicate the mean annual anomaly for the Northwest Atlantic (NWA). Colour bars indicate the relative contribution of each grouping unit to the mean anomaly. The black line indicate the overall trend across the NWA based on 3-y running average of annual mean anomalies. See Figs. 1 & 2B for the location of geographical grouping units, oceanographic sections and high-frequency monitoring sites.

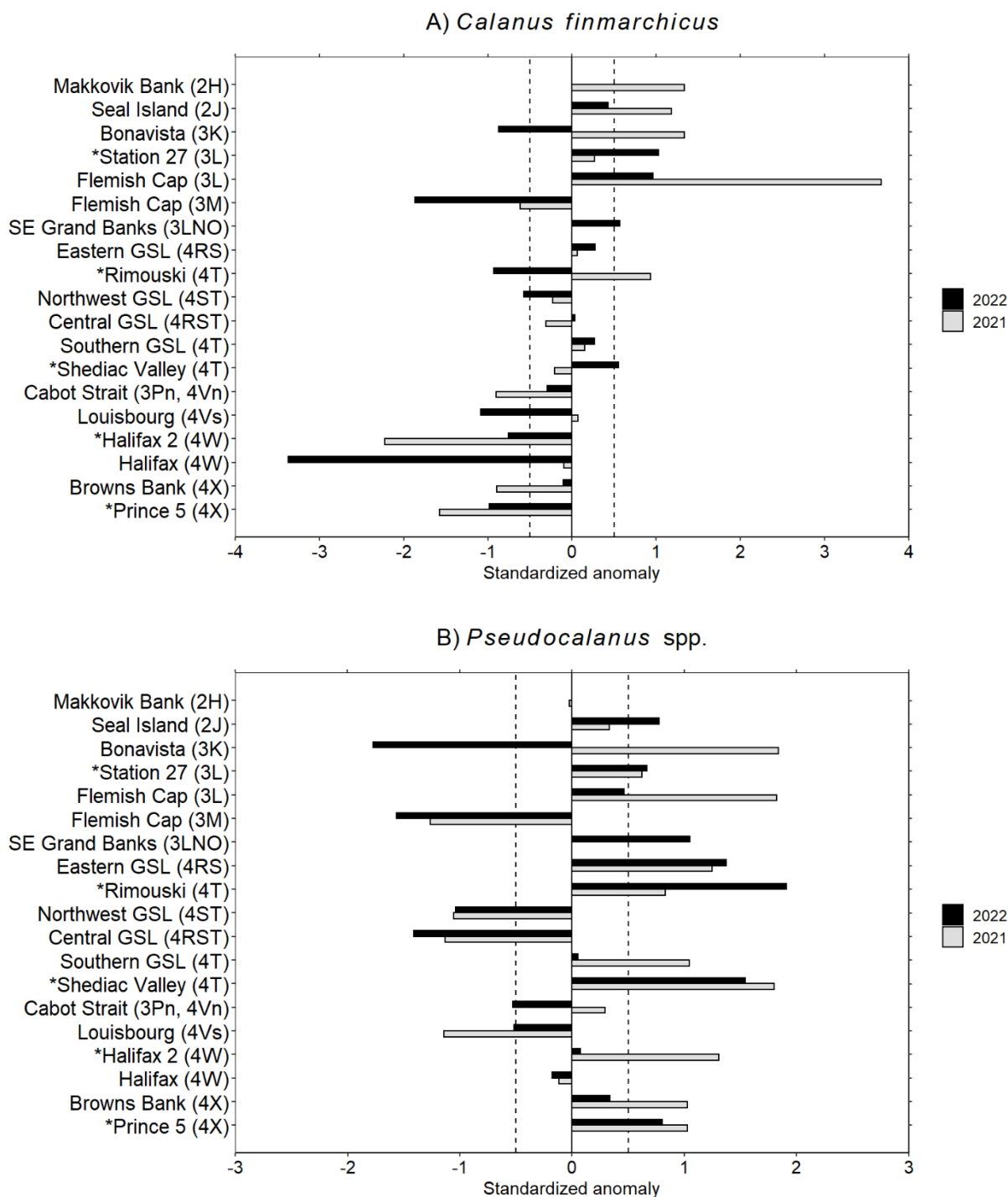


**Figure 10.** Comparison between 2021 and 2022 annual anomalies for (A) *Calanus finmarchicus*, and (B) *Pseudocalanus* spp. copepod abundance ( $\text{ind.} \cdot \text{m}^{-2}$ ) for each AZMP oceanographic section and high-frequency monitoring site sampled by the AZMP. Anomalies were calculated based on a 1999-2020 reference period. Anomalies within  $\pm 0.5$  SD (vertical dashed lines) are considered to represent near-normal conditions. Sampling locations are listed from north (top) to south (bottom). Asterisks (\*) indicate high-frequency monitoring sites. See Figure 2B for oceanographic sections and high-frequency monitoring sites location.

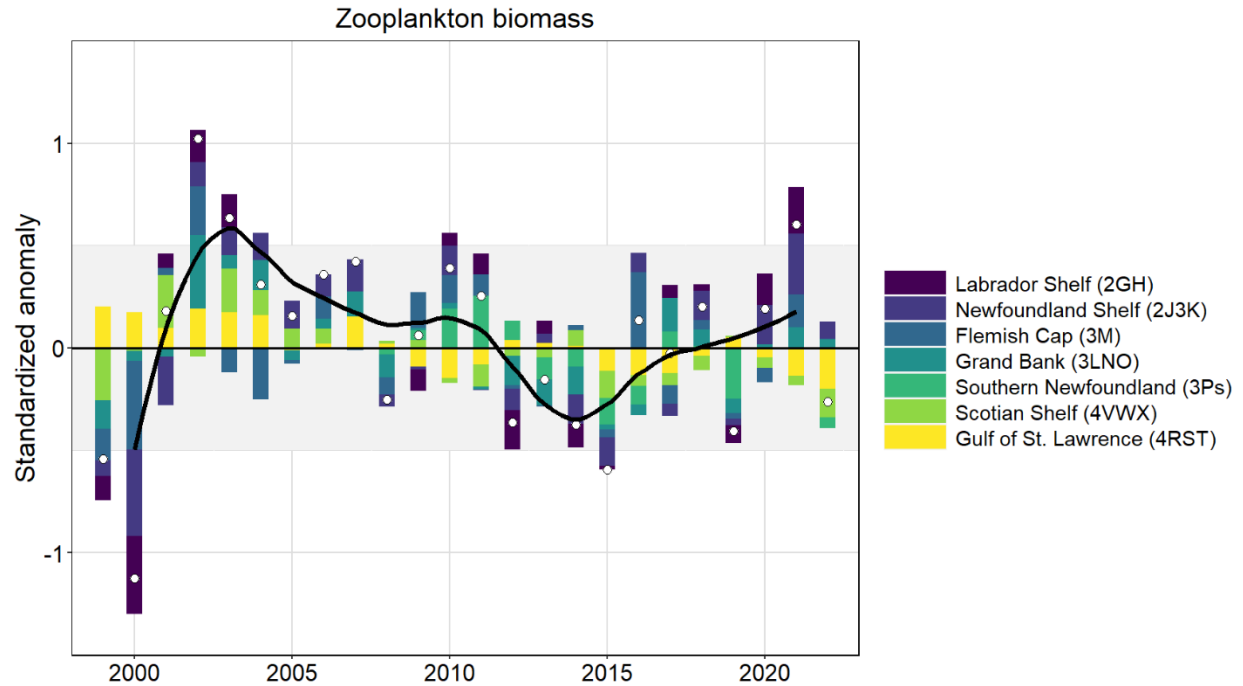


**Figure 11.** Annual anomaly time series of zooplankton biomass ( $\text{g dry weight} \cdot \text{m}^{-2}$ ) in six NAFO Ecological Production Units (EPU) and in the Gulf of St. Lawrence. Standardized anomalies were calculated for each oceanographic section and high-frequency monitoring site using a 1999-2020 reference period and averaged over geographical grouping units (EPUs or GSL). White circle indicate the mean annual anomaly for the Northwest Atlantic (NWA). Colour bars indicate the relative contribution of each grouping unit to the mean anomaly. The black line indicate the overall trend across the NWA based on 3-y running average of annual mean anomalies. See Figs. 1 & 2B for the location of geographical grouping units, oceanographic sections and high-frequency monitoring sites.



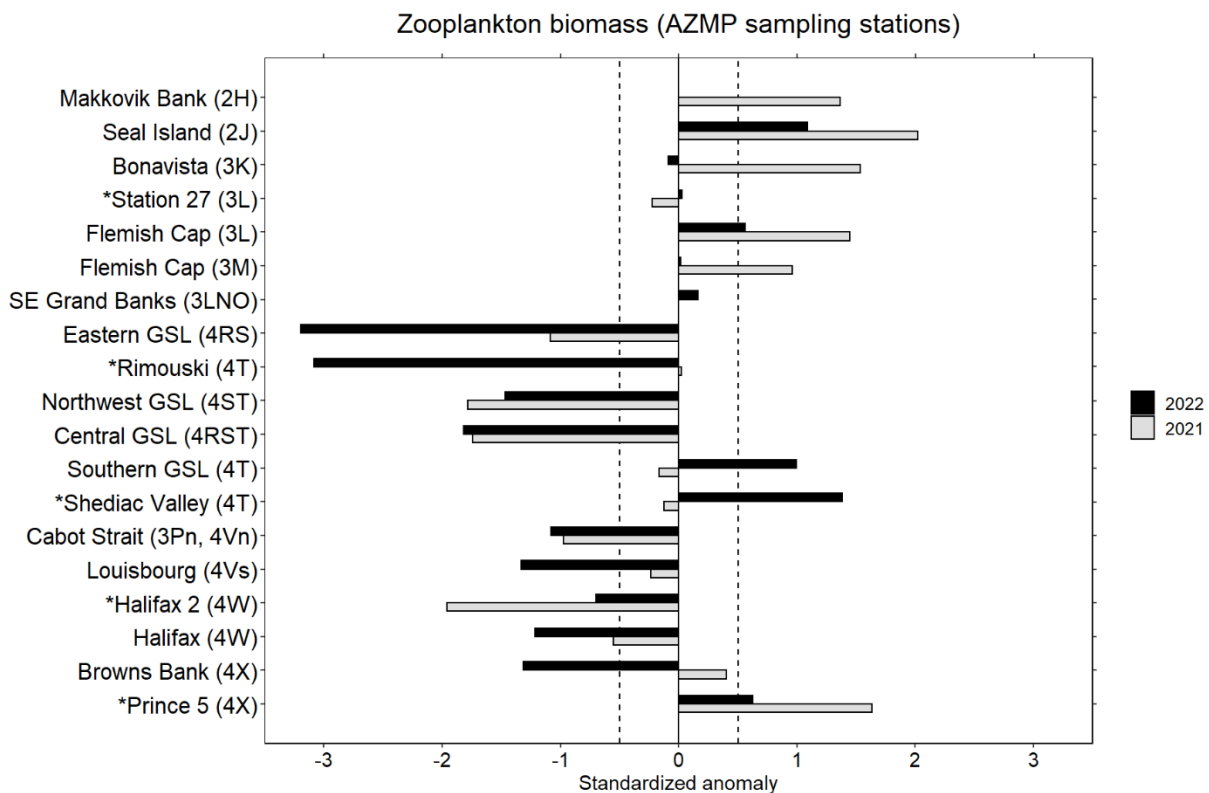


**Figure 12.** Comparison between 2021 and 2022 annual anomalies for zooplankton biomass ( $\text{g} \cdot \text{dry weight} \cdot \text{m}^{-2}$ ) for each AZMP oceanographic section and high-frequency monitoring site sampled by the AZMP. Anomalies are calculated based on a 1999-2020 reference period. Anomalies were calculated based on a 1999-2020 reference period. Anomalies within  $\pm 0.5$  SD (vertical dashed lines) are considered to represent near-normal conditions. Sampling locations are listed from north (top) to south (bottom). Asterisks (\*) indicate high-frequency monitoring sites. See Figure 2B for oceanographic sections and high-frequency monitoring sites location.

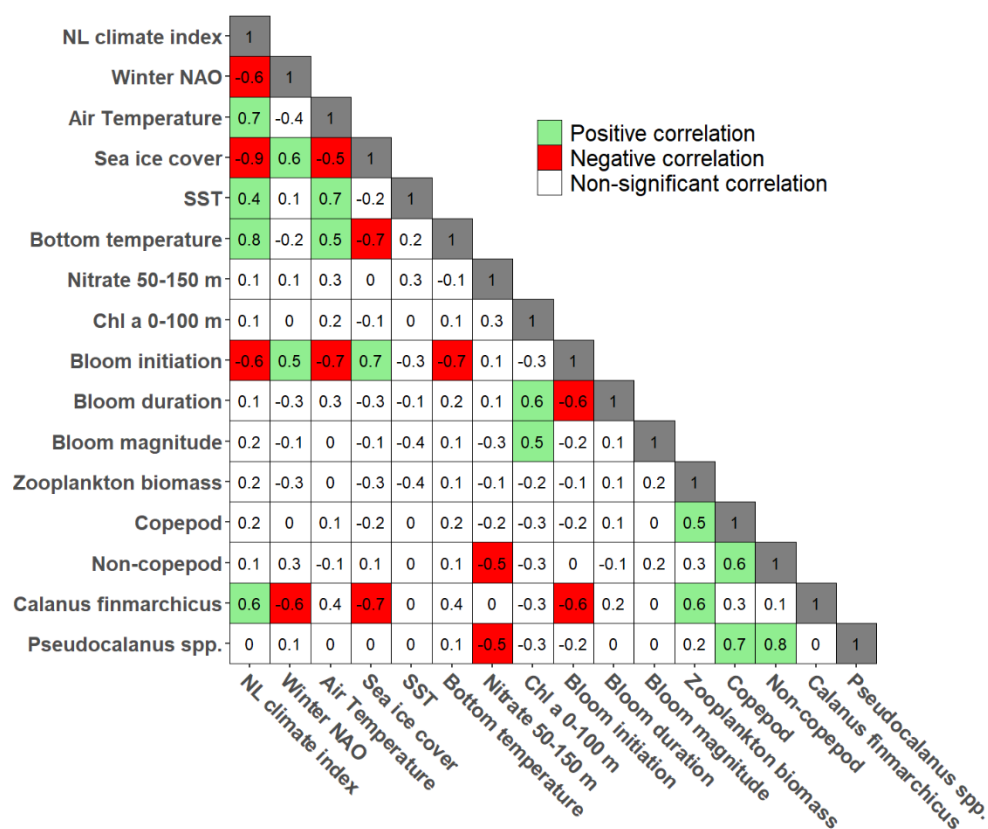


**Figure 13.** Correlation matrix summarizing the relationships between physical (Newfoundland and Labrador climate index, winter North Atlantic Oscillation [NAO] index, air temperature, sea ice cover, sea surface temperature [SST], and bottom temperature), and biogeochemical (phytoplankton spring bloom initiation, duration, and magnitude; integrated deep nitrate [50-150 m]; integrated chlorophyll *a* [chl *a* 0-100 m]; abundance of copepod, non-copepod, *Calanus finmarchicus*, *Pseudocalanus* spp.; zooplankton biomass) indices for the Southern Newfoundland, Grand Bank, Flemish Cap, Newfoundland Shelf, and Labrador Shelf EPU during the 1999-2022 period. Green cells indicate significant positive correlation, red cells indicate significant negative correlation, and white cells indicate non-significant correlations. Numbers in cells are Spearman correlation coefficients ( $\rho$ ). Significance level for Spearman correlation tests was  $\alpha=0.05$ .